Effect of axial electric field on the Rayleigh instability at small length scales

Darshak K. Bhuptani and Sarith P. Sathian[*]

Department of Applied Mechanics, Indian Institute of Technology - Madras, Chennai, Tamil Nadu, India

(Received 13 June 2016; revised manuscript received 8 December 2016; published 26 May 2017)

The effect of an electric field along the longitudinal axis of a nanoscale liquid thread is studied to understand the mechanism of breakup. The Rayleigh instability (commonly known as the Plateau–Rayleigh instability) of a nanosized liquid water thread is investigated by using molecular dynamics simulations. The breakup mechanism of the liquid nanothread is studied by analyzing the temporal evolution of the thread radius. The influence of the temperature of the liquid nanothread and the electric-field strength on the stability and breakup is the major focus of the study. The results show that the axial electric field has a stabilizing effect even at nanoscale. The results from the simulations are in good agreement with the solutions obtained from the dispersion relation developed by Hohman *et al.* for the liquid thread. The critical electric-field strength necessary to avoid the breakup of the liquid thread is calculated and other effects such as the splaying and whipping instability are also discussed.

I. INTRODUCTION

There is renewed interest in the stability of a liquid jet or a liquid thread at small length scales due to its important role in novel applications such as drug delivery systems [1], electronic cooling [2], ink-jet printing [3,4], nanoscale machining [5], production of fine threads of fibers [6], etc. Studies on the stability of a liquid jet and thread structure possess a long history beginning with Savart [7], who observed that the breakup of a liquid jet occurs spontaneously and thus is a property of the jet dynamics. Later, Plateau confirmed through his experiments that the instability magnifies on the jet surface when the length of a liquid column exceeds the diameter by a factor varying between 3.13 and 3.17. Rayleigh [8] was the first to derive a mathematical description for the stability of a liquid jet by analyzing the temporal evolution of the small perturbations on the liquid column (thread) surface. It was concluded that the disturbance grows or decays exponentially due to surface tension with the most unstable dimensionless wave number of 0.697. The liquid tries to reduce the surface energy with the fastest growing wavelength which is about nine times the radius of jet or thread leading to the breakup. The effect of the viscosity of the liquid thread and its surrounding was taken into consideration by Tomotika [9], who found that the viscosity has a damping effect and thus stabilizes the liquid jet or thread. The theoretical expression predicts the most unstable dimensionless wave number to be 0.568 and a similar wave number was reported experimentally by Taylor [10] for similar conditions.

The early experimental work by Zeleny [11] on the instability of electrified liquid surface found that the instability can be manipulated by using an electric field. The effect of an axial electric field on the stability of a liquid column was studied analytically by Nayyar and Murty [12], who found that the axial electric field has a stabilizing effect. Experimental studies by Raco [13] and Taylor [14] have also shown that the Plateau–Rayleigh (varicose) instability can be completely suppressed with the moderate axial field strengths. Analytical studies by Saville [15] have shown that the axial field can

completely suppress the Plateau–Rayleigh instability and the stabilization for leaky dielectric liquid are at lower electric-field strength compared with the perfectly dielectric liquids. Sankaran and Saville [16] have also shown that an axial electric field which stabilizes a liquid column of fluid A immersed in surrounding B but can destabilize the same combination if the fluids are interchanged respectively. A simple mathematical model describing the stability of an axisymmetric jet in the presence of an axial electric field was derived by Hohman *et al.* [17]. This resulted in a simple generic algebraic equation, commonly known as the dispersion relation, relating the growth rate and the wavelength of the disturbance imposed on the liquid thread surface. This dispersion relation is a general equation which is valid for the fluids with any value of viscosity, surface tension, conductivity, and surface charge density. The solution obtained from this dispersion relation is comparable with Rayleigh's solution for the inviscid fluid thread in the absence of electric field, conductivity, and the surface charge. In the presence of an axial electric field, the solution (dispersion curves), i.e., the growth rate for different reduced wave number, are very similar to that of the reported dispersion curves by the Saville [15] for various electric-field strengths under similar physical conditions.

These studies have shown the importance of the surface tension, viscosity, ambient conditions, and electric-field strength on the stability of a macroscale liquid thread or jet. To understand the stability and the breakup mechanism of a nanoscale liquid thread, Koplik and Banavar [18] used molecular dynamics (MD) simulations and reported that the rupture time of these threads (short nanothread) are of the same order of magnitude as predicted by Rayleigh. Kawano [19] studied the rupture of the liquid argon nanothread using MD simulations and found that the dimensionless wave number leading to the breakup is close to the value predicted by the inviscid linear stability theory for a fluid column. Studies on the breakup of nanoscale liquid jets by Moseler and Landman [20] have shown the emergence of a new breakup profile known as double-cone profile leading to the symmetric pinch-off. This study has shown the importance of the thermal fluctuations at small length scales and considered as a competing force which is comparable to the surface tension force. Thermal fluctuations were included in the lubrication
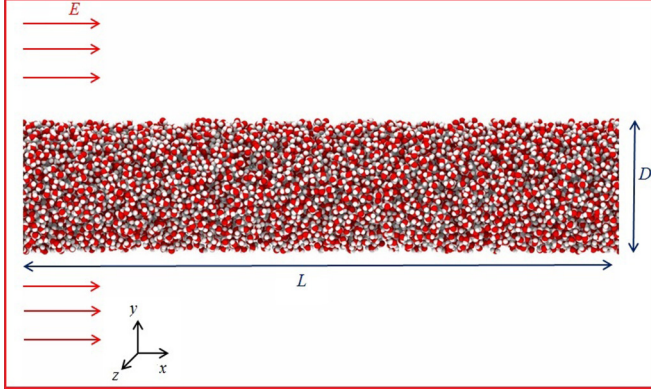
———
[*]sarith@iitm.ac.in

FIG. 1. Schematic of the simulation box elucidating the general configuration of water molecules with length (L) and diameter (D) in the presence of an axial electric field (E). The figure is not to scale.

TABLE I. The simulation parameters employed in this study.

Parameter	Value
van der Waals radius, σ_{OO}	0.3166 [nm]
$\sigma_{OH}; \sigma_{HH}$	0.0 [nm]
Well depth, ε_{OO}	0.1553 [kcal/mol]
$\varepsilon_{OH}; \varepsilon_{HH}$	0.0 [kcal/mol]
Charge on atom, $q_O; q_H$	$-0.8476; 0.4238$
Bond length between O & H atom	0.1 [nm]
Angle between O–H bonds	109.47°
Number of water molecules	2400 ($r = 0.5$ nm) to
	38 000 ($r = 2$ nm)
Equilibration run time step	0.025 [fs]
Total equilibration run	1.25 [ps]
Production run time step	0.25 [fs]
Total production run	262.5 [ps]

equation (modified Navier–Stokes equation) describing jet or thread mathematically by Moseler and Landman and the results were compared with the MD simulations. Analytical work by Eggers [21] have also confirmed the role of the thermal fluctuations and found by using the path integral method that the most probable breakup mode has a self-symmetric profile. Kang and Landman [22] have explored the effect of environmental conditions on the breakup process and profiles for the liquid nanobridges. The study concluded that the environmental conditions can modify the breakup process as well as the breakup profile. Tiwari *et al.* [23] studied the breakup of a liquid jet or thread by using dissipative particle dynamics (DPD) and studying the temporal evolution of the minimum thread radius near the pinch-off point, confirming the role of thermal fluctuations at nano length scales. A study by Gopan and Sathian [24] has shown that the breakup of a liquid nanothread is initiated by the surface tension and that thermal fluctuations accelerate the breakup at the later stage of a breakup process only when the radius of a nanothread is comparable to its thermal length scale.

Studies to date have improved our understanding of the stability and breakup of liquid nanothreads. However, the stability of nanoscale structures of polar liquids in the presence of an axial electric field is not well understood. The aim of this study is to investigate how the applied axial electric field affects the stability and breakup of liquid threads placed in vacuum at small length scales. The role of thermal fluctuations in the breakup and stability of the nanothreads is known but its influence on the stability in the presence of an axial electric field is not yet explored. Simulations are also performed to understand the influence of liquid thread temperature on the stability and its breakup without the electric field.

II. SIMULATION DETAILS

The simulation box (Fig. 1) which measures 260 nm × 20 nm × 20 nm in the x, y, and z directions respectively, consists of a liquid water thread [parameters are chosen to be that of the extended simple point charge (SPC/E) water model] which is time integrated by using the velocity Verlet algorithm. The water molecules for each simulation are arranged in the cylindrical shape to have an approximate density of

1000 kg/m^3. The timescale τ for a SPC/E water molecule is given by $\tau = \sqrt{m\sigma^2/48\varepsilon}$ where m is the mass of a water molecule, and σ and ε are the Lennard–Jones potential for the SPC/E water model. Seven cases of liquid threads with a length L of 90 nm and radii r of 0.5, 0.75, 1 nm, 1.25, 1.5, 1.75, and 2 nm are simulated. The aspect ratio (L/r) of these threads varies from 45 to 180. To study the effect of the liquid thread temperature on its stability and breakup, equilibrium MD (EMD) simulations are performed, while to understand the effect of electric fields, nonequilibrium MD (NEMD) simulations are employed. All MD simulations are performed by using LAMMPS [25] and property evaluations are done by postprocessing the MD trajectory by using the codes developed for this purpose. Visualization of the MD trajectory is done by using OVITO [26]. The conjugate-gradient algorithm is used to minimize the potential energy of the system. The thread is equilibrated to the desired temperature by using canonical ensemble (NVT) where the temperature is maintained by using a Nosé–Hoover thermostat with a time step of 0.001τ. The production run consists of a time evolution of the system as per the microcanonical ensemble (NVE) with a time step of 0.01τ. The bond length and the bond angle are held constant throughout the simulations by using the SHAKE algorithm. The details of the parameters employed in the present study are shown in Table I. The equilibration curves for a nanothread of length 90 nm and radius 1 nm at 300 K are shown in Fig. 2. A similar exercise was carried out for all the thread radii. In all cases considered, an equilibration time of 1.25 ps is found to be sufficient. At the nanoscale, no external perturbation is applied on the thread surface because this is initiated due to the presence of the thermal fluctuations inherently which is seen during the equilibration process [24].

To understand the time evolution of the nanothreads and the associated dynamics for various physical conditions, the value of viscosity and surface tension are to be made known for each condition. The role of viscosity in the jet or thread breakup dynamics is to reduce the growth rate of the perturbation imposed on the thread surface [9], while the surface tension increases the growth rate of the perturbation in order to reduce the surface energy [8]. Thus, the thread viscosity stabilizes the liquid jet or thread while the surface tension
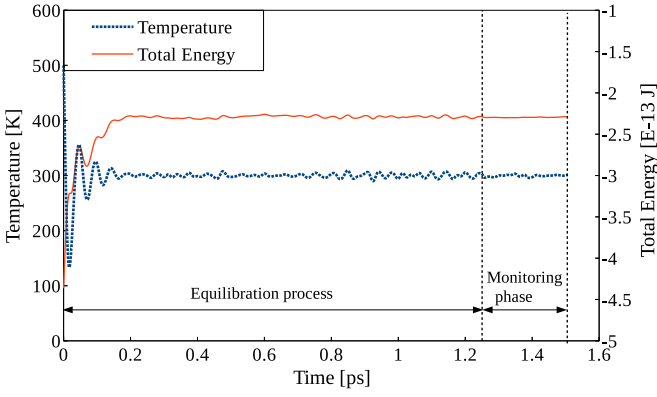
FIG. 2. Equilibration curves for a nanothread of length 90 nm and radius 1 nm at 300 K (Case 10; see Table III).

TABLE II. Shear viscosity and surface tension of liquid water at various temperatures with 125, 1000, 3375, and 8000 water molecules in the system.

SI. no.	Temperature [K]	Shear viscosity [mPa. s]	Surface tension [mN/m]	Length scale [nm]
1	280	0.3918	61.58	0.2505
2	300	0.3144	57.02	0.2695
3	320	0.2575	53.02	0.2886

tends to destabilizes it. To validate the inviscid assumption in our studies, so as to compare with the classical Rayleigh prediction, the Ohnesorge number Oh, which is defined as the ratio of viscous forces to inertial and surface tension forces, is evaluated. If Oh $\ll$ 1, the effect of viscosity while determining the dynamics of the thread can be safely neglected. To estimate the viscosity of liquid water, separate equilibrium simulations are performed by using the Green–Kubo (G-K) method [27] at temperatures of 280, 300, and 320 K. The shear viscosity is defined as

$$\mu = \frac{V}{k_B T} \int_0^\infty \langle P_{xy}(0) P_{xy}(t) \rangle dt, \qquad (1)$$

where V is the volume of the system and P_{xy} are the off-diagonal components of the pressure tensor that is calculated from the EMD simulations. To evaluate the surface tension of liquid water, test area simulation method (TASM) [28] is employed. At nanoscale, shear viscosity depends on the number of water molecules presents in the system [24]. Thus, to ensure that the simulation box size and the number of water molecules have minimal effects on the viscosity, equilibrium MD simulations are performed with 125, 1000, 3375 and 8000 water molecules for 2 ns. The simulation box size for calculating dynamic viscosity are the cubes with each side measuring 1.55, 3.1, 4.65, and 6.2 nm, respectively. The number of water molecules and the simulation box size are chosen so as to have an approximate density of liquid water as 1000 kg/m³. For TASM, the cubical simulation box is converted into a rectangular cuboid along the z direction (symmetric about xy plane) such that vacuum-liquid interface is allowed to form at both ends of the bulk liquid. The mean viscosity and surface tension of liquid water at three temperatures are shown in Table II and are in good agreement with the reported values at the same temperature [29,30]. In the present study, Oh is found to be either greater than or approximately equal to unity for various values of thread radii, dynamic viscosity, and surface tension considered. Thus, the viscous effect cannot be neglected while analyzing the dynamics of the thread, so the inviscid assumption is not valid in the present study. The surface charge density and the conductivity of the liquid thread are taken to be zero for all the cases because no free charges are introduced in the

simulations. The thermal length scale is also evaluated at the respective temperature, which is defined as $l_T = \sqrt{k_B T / \gamma}$.

To study the breakup mechanism and the role of different forces involved in determining the stability, the temporal evolution of the nanothread radius has to be investigated. Following the work of Kang *et al.* [22], the simulation box is sliced into rectangular bins with a bin size of 1 nm along the thread axis (x axis). The center of mass for each bin is calculated by the mass balance in the y and z directions. Each bin is radially divided with 0.05 nm thickness by using the center of mass as the center of the liquid thread. The interface is identified as the radial bin where the density is less than 20% of the core density of the liquid thread. The average radius is calculated by identifying all the atoms present at the interface and measuring its distance from the center of mass. The process is repeated at every 5000 steps (1.25 ps) to get the temporal variation of the thread radius for the first breakup.

In the MD simulations, electric field is introduced in such a way that an additional force is applied on each atom (particle) [25,31], and thus the modified potential is given as

$$U_{LJ}(r_{ij}) = 4\varepsilon_{ij}\left[\left(\frac{\sigma_{ij}}{r_{ij}}\right)^{12} - \left(\frac{\sigma_{ij}}{r_{ij}}\right)^6 \right] + \frac{k_c q_i q_j}{r_{ij}} + q_i E, \qquad (2)$$

where ε_{ij} is the depth of the potential well, σ_{ij} is the interparticle distance at which potential energy is zero, r_{ij} is the distance between two particles, k_c is the electrostatic constant, q is the charge of that particular atom, and E is the applied electric-field strength. The first term on the right-hand side of Eq. (2) describes the van der Waals interaction between the atoms. The second term describes the long-range Coulombic interaction due to the partial charges on the oxygen and the hydrogen atoms of the water molecules. The third term denotes an additional external force due to the applied electric-field strength along the thread axis (x direction). Depending on the partial charge of the atom (hydrogen or oxygen) an additional force on each atom is added along the direction in which electric field is desired to be applied.

Because water molecules are polar in nature, the effect of the water molecules on the electric field is also considered. In the presence of an applied electric field, the water molecules get displaced, and thus the distance between two individual molecules changes. This effect is reflected in the system dynamics by the van der Waals and long-range Coulombic interactions.

III. INSTABILITY OF LIQUID THREAD IN PRESENCE OF AXIAL ELECTRIC FIELD

A mathematical model describing the physical mechanism of the instability of a liquid jet in the presence of an axial electric field has been derived by Hohman *et al.* [17]. The solution of this mathematical model reduces to the classical Rayleigh case [8] and the cases considered by Saville [32] under appropriate conditions and simplifications. The breakup of a liquid thread is initiated due to the pressure difference across the thread surface in order to minimize the surface energy by reducing the surface area. The pressure difference across the charged liquid surface in the presence of an axial electric field [17] is

$$\Delta p = \gamma \kappa - \frac{\varepsilon - \overline{\varepsilon}}{8\pi} E^2 - \frac{2\pi}{\overline{\varepsilon}} \sigma^2, \tag{3}$$

where κ is the mean curvature of the interface, γ is the surface tension of the fluid, ε is the fluid dielectric constant, $\overline{\varepsilon}$ is the ambient dielectric constant, and σ is the surface charge density. In the absence of an electric field and the surface charge, the above equation reduces to the Young–Laplace equation for the pressure difference across the interface. In the above Eq. (3), the electrostatic term proportional to E^2 indicates the energy difference across the interface between the thread and the surroundings. The term proportional to σ^2 contributes to the radial self-repulsion of the free charges on the surface. In the absence of the free charges on the surface, the electrical force balances the surface tension force for the constant pressure across the interface.

The dimensionless governing equations are obtained by selecting appropriate nondimensional parameters such as $t_0 = (\rho r^3/\gamma)^{1/2}$, electric field $E_0 = \sqrt{\gamma/[(\varepsilon - \overline{\varepsilon})r]}$, and surface charge density $\sigma_0 = \sqrt{\gamma \overline{\varepsilon}/r}$. The jet/thread parameters are nondimensionalized as $\beta = \varepsilon/\overline{\varepsilon} - 1$, kinematic viscosity as $\nu^* = \sqrt{l_v/r}$ (where viscous length scale is $l_v = \rho \nu^2/\gamma$), gravity as $g^* = g\rho r^2/\gamma$, conductivity as $K^* = K(\rho r^3/\gamma\beta)^{1/2}$, and aspect ratio as $\chi = L/r$. The dimensionless asymptotic field as $\Omega_0 = E/E_0$. For comparing the dimensionless asymptotic field and Saville's electric field, the relationship between these two parameters is given as $\Omega_0^2 = 4\pi\beta E$. By using linear stability analysis, the general dimensionless dispersion equation describing the physical behavior of a liquid thread in the presence of an axial electric field is obtained [the dispersion relation (4) is from Ref. [17]] as

$$0 = \omega^{*3} + \omega^{*2}\left[\frac{4\pi K^* \Lambda}{\delta\sqrt{\beta}} + 3\nu^* k^{*2}\right]$$
$$+ \omega^*\left[3\nu^* k^{*2}\frac{4\pi K^* \Lambda}{\delta\sqrt{\beta}} + \frac{k^{*2}}{2}(k^{*2} - 1)\right.$$
$$+ 2\pi\sigma_0^2 k^{*2}\left(\frac{8\Gamma}{\delta} - 1\right) + \frac{\Lambda}{\delta}\frac{\Omega_0^2}{4\pi}k^{*2}\right]$$
$$+ \frac{4\pi K^* \Lambda}{\delta\sqrt{\beta}}\left[\frac{k^{*2}}{2}(k^{*2} - 1) + 2\pi\sigma_0^2 k^{*2}\right.$$
$$+ \frac{\delta\Omega_0^2}{\Lambda 4\pi}k^{*2} + \frac{E_0\sigma_0}{\sqrt{\beta}}ik^*\left(\frac{1}{\Gamma} - 4\right)\right], \tag{4}$$

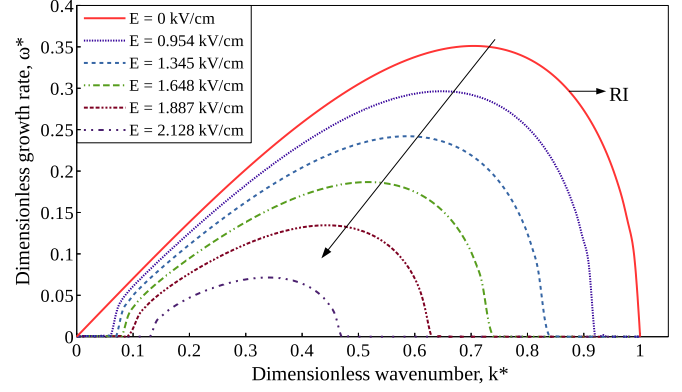where $\Gamma = \ln(1/\chi)$, $\Lambda = \beta \ln(1/\chi)k^{*2}$, and $\delta = 2 + \Lambda$.

FIG. 3. Dispersion relation for a zero-viscosity fluid as a function of E for $\beta = 77$.

If any one of the three roots or the real part of the complex root is positive, i.e., $\omega^*(\text{real}) > 0$, instability occurs. Solutions for the dimensionless growth rate (ω^*) of the disturbance imposed on the liquid thread surface for all dimensionless wave number (k^*) are obtained for a model of a deionised water jet of 1 mm diameter for various electric-field strengths. The resulting dispersion curves are in good agreement with the result reported for various values of E [8,17,32]. If the electric field, conductivity, and the surface charge density are ignored, then the solution of dispersion relation reduces to the classical Rayleigh instability (RI) dispersion curve, as shown in Fig. 3. The maximum growth rate for the zero electric-field strength occurs for the most unstable dimensionless wave number of 0.7 which agrees with Rayleigh's predicted value of 0.697.

From Fig. 3, it can be seen that an axial electric field has a stabilizing effect on the Rayleigh instability by reducing the maximum growth rate and the most unstable wave number [12]. The critical electric-field strength is comparable with the experimental value for a water jet of 1 mm diameter (≈ 2 kV/cm) [17]. By utilizing the solution of the dispersion relation, the critical (minimum) electric-field strength required to prevent breakup can be predicted for the minimum growth rate.

At the nanoscale, the fluid properties such as viscosity and surface tension may depend on the applied electric field. To evaluate these properties, the G-K and TASM methods described above are employed for the various electric-field strengths. Figure 4 shows that with an increase in the electric-field strength, the viscosity decreases and the maximum reduction in the viscosity is approximately 17% for a field strength of 1 V/nm. The observed change in the viscosity of liquid water is not much appreciable and, therefore, the effect of electric field on the viscosity of liquid water can be neglected. At the macroscale, the influence of electric field on surface tension is negligible [33,34] but, at the nanoscale, the increase in surface tension is appreciable (approximately 52% for 0.3 V/nm), as observed in Fig. 5.

IV. RESULTS AND DISCUSSION

A. Nature of breakup process

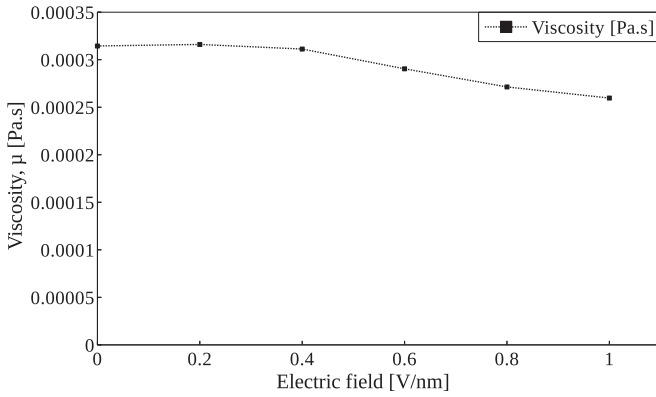Molecular dynamics simulations enabled the visualization of the time evolution of a liquid nanothread giving us the

FIG. 4. Effect of electric field on the dynamic viscosity of liquid water.

FIG. 6. Temporal evolution of the minimum thread radius with the initial thread radius as 1 nm at 300 K.

insights on its dynamical behavior. The visualization (for the case of a liquid nanothread placed in a vacuum without electric field) revealed that the breakup points are irregular in space and time. This is exactly opposite in nature to the macroscopic case, where the breakup is spatially spaced and two connecting beads (forming drops) are connected by a thin thread which eventually leads to the formation of the satellite (secondary) drops [24,35]. At the nanoscale, satellite droplet formation is also not seen (as seen in left panels of Figs. 10 and 13, respectively), and the drops are approximately monodispersed (as reported in previous studies [19,24]) whereas it is polydispersed for macroscale thread breakup [35]. This is attributed to the symmetrical double-cone breakup profile which is observed at the nanoscale [20]. Previous studies [20,21,35] have shown that the nature of the breakup process can be identified either as a deterministic or a stochastic process. Following the work of Tiwari *et al.* [23], the nature of the breakup process at the nanoscale is explored by analyzing the temporal evolution of the minimum radius ($r_{\min}$) around the pinch-off point. The minimum radius is dependent on the breakup time for both deterministic and stochastic pinching [21,23] and is given by
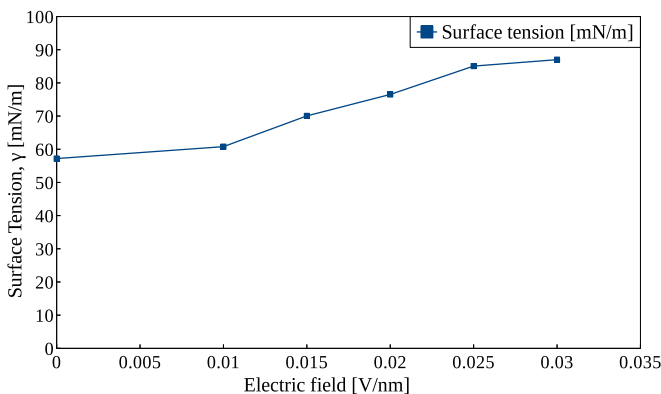
$$r_{\min} = C(T - t)^{\alpha}, \tag{5}$$

FIG. 5. Effect of electric field on the surface tension of liquid water.
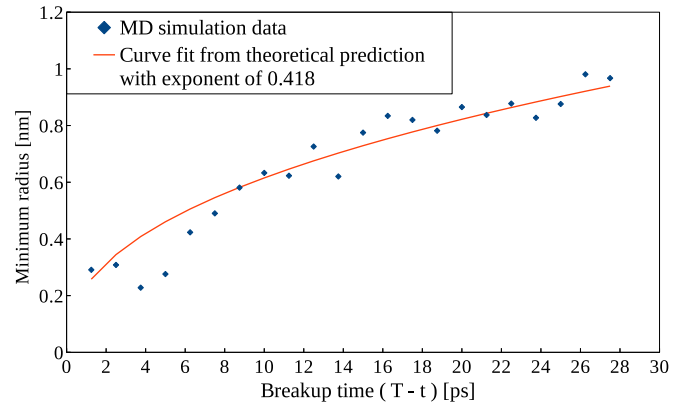
where C is a constant which depends on the viscosity, density, and surface tension of the liquid, T is the total breakup time, t is the local time just before the breakup, and α is an exponent determining the type of pinching process. In the case of deterministic pinching, the value of α is close to unity [35], while for the stochastic pinching, it is equal to 0.418 [21]. The thermal fluctuation is the reason behind the symmetrical pinching [20] making the surface tension force irrelevant. The temporal evolution of the minimum radius for the first pinch-off is shown in Fig. 6, where the initial radius is 1 nm and length 90 nm of the liquid thread at 300 K. This confirms the earlier observations [21,23,24] that the initial stages of the breakup process are driven by the surface tension forces and, only at the later stages, when the minimum radius is comparable to the thermal length scales, do thermal fluctuations dominate and accelerate the breakup process.

B. Effect of temperature on stability

According to the Rayleigh instability theory, perturbation given to the liquid surface has all sets of wavelengths which may either grow or decay in time. The wave number for the maximum growth rate of these perturbations decides the number of droplets that can be formed for a liquid thread. There will be only one wavelength which dominates over all other wavelengths that lead to the breakup. The effective wavelength is calculated as the initial thread length divided by the maximum number of droplets formed, because they have a natural tendency of coalescing with each other to form a single drop. The dimensionless wave number (kr) is given as [19,24]

$$k^* = kr = \frac{2\pi r}{\lambda} = \frac{2\pi r N}{L}, \tag{6}$$

where λ is the effective wavelength, r is the initial thread radius, N is the maximum number of drops formed, and L is the initial length of the thread. The dimensionless wave number for the nanoscale threads are found to be in the range of 0.1 to 0.5, as shown in Table III, and it is in good agreement with the results from similar studies [19,24]. It may be noted that, with an increase in temperature, the viscosity and the surface tension decreases while the thermal length scale increases, leading to a reduction in the first breakup time. The variation

TABLE III. Results of MD simulation and solutions from dispersion relation for various thread radii at 280, 300, and 320 K.

Case	Radius [nm]	Temp. [K]	MD Simulation results			Solutions from dispersion relation (4)		
			Breakup time [ps]	No. of drops formed N	Dimensionless wave number kr	No. of drops formed N	Dimensionless wave number kr	Critical electric field [kV/cm]
1	0.5	280	16.5	9	0.314	8.59	0.30	3000
2	0.75	280	20.0	4	0.210	6.11	0.32	2400
3	1.0	280	87.5	4	0.279	4.87	0.34	2100
4	1.25	280	108.75	3	0.261	4.01	0.35	1900
5	1.5	280		1	0.104	3.53	0.37	1700
6	1.75	280		1	0.122	3.11	0.38	1600
7	2.0	280		1	0.139	2.79	0.39	1500
8	0.5	300	14.5	9	0.314	9.16	0.32	2900
9	0.75	300	18.75	6	0.314	6.49	0.34	2300
10	1.0	300	27.5	5	0.349	5.15	0.36	2000
11	1.25	300	96.25	3	0.261	4.35	0.38	1800
12	1.5	300	102.5	3	0.314	3.72	0.39	1600
13	1.75	300	202.5	2	0.244	3.27	0.40	1500
14	2.0	300		1	0.139	2.93	0.41	1400
15	0.5	320	10.25	14	0.488	9.74	0.34	2800
16	0.75	320	14.75	6	0.314	7.06	0.37	2300
17	1.0	320	26.25	5	0.349	5.58	0.39	2000
18	1.25	320	97.5	4	0.349	4.58	0.40	1800
19	1.5	320	82.5	3	0.314	3.91	0.41	1600
20	1.75	320	171.25	2	0.244	3.43	0.42	1500
21	2.0	320		1	0.139	3.08	0.43	1400

of the first breakup time for the various thread radii at three values of temperatures is shown in Fig. 7. It should be noted that a faster breakup does not mean simultaneous breakup. The simulations reveal that the multiple breakups are temporally spaced. The breakup of thread creates new free surfaces which modify the breakup process further.

From a molecular perspective [24], the surface tension is the net force due to the potential energy, i.e., molecular interactions. As the temperature of the liquid thread increases, the kinetic energy of all the molecules increases while surface tension (potential energy) decreases, which results in the increased number of breakup points per unit length [24]. Thus, the number of drops formed increases with an increase in the thread temperature (Fig. 8)

C. Application of linear stability analysis in presence of electric field at small length scales

The applicability of a dispersion relation (4), which was developed by Hohman *et al.* [17], to the nanoscale regime would be highly relevant to be investigated. To verify this, solutions are obtained for the cases described by Kawano [19] by using MD for the breakup of a liquid argon nanothread. The aspect ratio of the nanothreads in Kawano's studies varied from 30 to 130 while, for the present study, it varies from 45 to 180. The comparison of the dimensionless wave number (k^* or kr) and the maximum number of droplets (N) formed is shown in Table IV, which is obtained from the solution of the dispersion relation under similar conditions mentioned in Kawano's studies. It can be seen that the
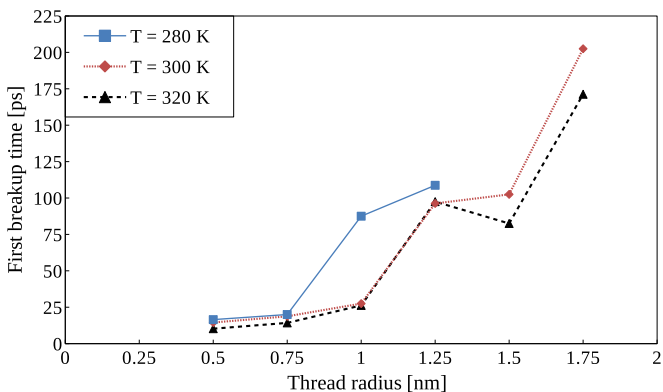

FIG. 7. First breakup time for the three temperatures studied for various thread radii.
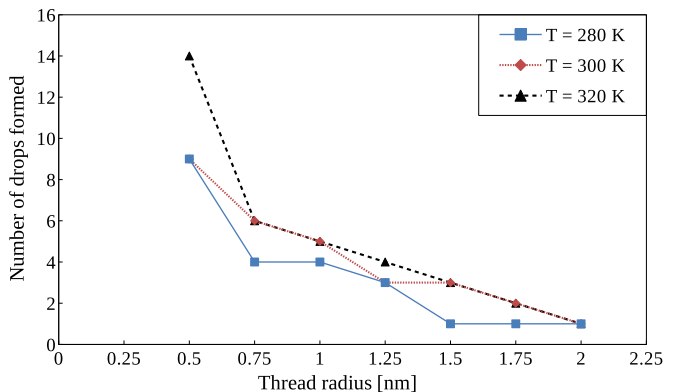

FIG. 8. Number of drops formed for the three temperatures studied for various thread radii.

TABLE IV. The results from MD simulation presented in Ref. [19] and the solutions obtained by using dispersion relation (4) for the same cases under similar physical conditions.

	L	R	MD results		Solutions of Eq. (4)	
Case	[nm]	[nm]	kr	N	kr	N
1	14.16	0.2789	0.433	3–4	0.29	2.344
2	28.32	0.3752	0.5	6	0.31	3.725
3	42.48	0.3324	0.418	8–9	0.3	6.108
4	42.48	0.8673	0.386	3	0.36	2.807
5	42.48	1.3522	0.4	2	0.39	1.95

dispersion relation is able to predict fairly accurately when the radius of a nanothread is greater than the thermal length scale (0.3375 nm for Kawano's study). During the equilibration process, the radius of a nanothread decreases from its initial value due to the vaporization of the surface molecules from the core liquid. The equilibrium radius thus reached is considered for obtaining the solution from the dispersion relation. It is to be noted that the dispersion relation does not account for the thermal fluctuations.

For the present study the electric field is considered (neglecting the conductivity and surface charge density) while solving the dispersion relation to get the dispersion curves. The values of critical electric-field strength for various thread radii at 280, 300, and 320 K are obtained from the dispersion curves. As an example, dispersion curve for the Case 10: $L = 90$ nm and $r = 1$ nm at 300 K is presented in Fig. 9. This is obtained for various values of E for which the growth rate is either zero or negative. This gives a clear indication of the critical electric-field strength required to stabilize and prevent the breakup of the nanosized liquid thread.

Table III shows the results of the simulations for the cases without electric field and the corresponding solutions. The value of critical-field strength is used as an input to the MD simulation to study the effect of an axial electric field on the stability of a liquid nanothread. The visualization of the resulting MD trajectories shows that the liquid thread does not undergo any breakup but instead coalesces into a single drop. When the radius is less than 1 nm, the thread breaks
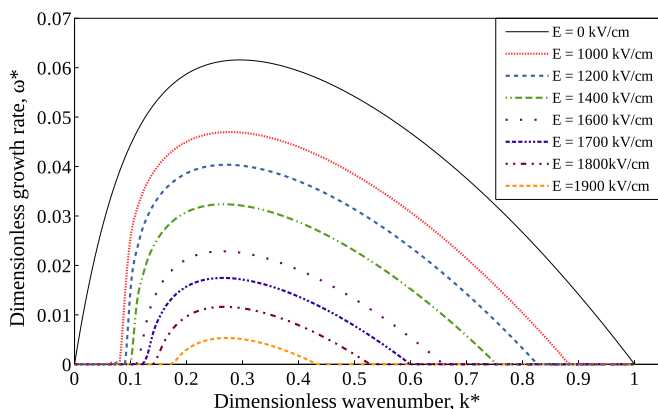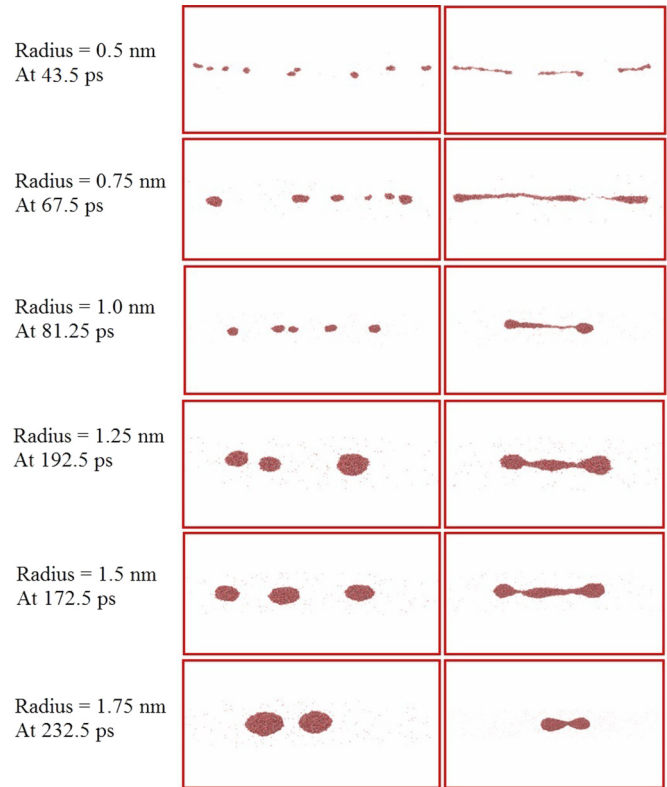

FIG. 10. Snapshots of MD trajectory from Case 8 to Case 13 (Table III) (left column indicates the cases without electric field and the corresponding cases with critical electric-field strength predicted from the solution of the dispersion relation is on the right column).

but the number of breakup points are less compared with a case without electric field. The snapshots of MD trajectory in the absence and presence of an axial electric field at the same time instants are shown in Fig. 10. For a given radius and for the same time elapsed, the maximum number of droplets formed are compared for both the cases.

The observed results indicate that, even at the nanoscale, an axial electric field has a stabilizing effect by preventing the breakup. MD simulations reveal that, only when the thread radius is greater than 1.75 nm does it coalesces into a single large droplet in the absence of an electric field for all three temperatures considered in this study. This is because of the long-range electrostatic interaction which prevents the liquid thread from undergoing breakup. In the presence of an electric field, the liquid nanothread does not undergo any breakup and coalesces into a single drop by the end of the production run. A complete temporal evolution for Case 10: $L = 90$ nm and $r = 1$ nm at 300 K with an axial electric-field strength of 2900 kV/cm is presented in Fig. 11 from 0 to 200 ps. Similar behavior is observed for all cases considered in the present study. The critical field strength calculated from the dispersion relation and that obtained from the MD simulations are compared (Fig. 12). It is observed that the strength of the electric field required for suppressing the Rayleigh instability increases with a decrease in the thread radius. This could be due to the work that has to be done by the electrical force against the molecular interaction and the dipole moment. The SPC/E water molecule has a net polar dipole moment ζ of

FIG. 9. Dispersion curves for Case 10 ($L = 90$ nm and $r = 1$ nm at 300 K) for various electric-field strength, E, and $\beta = 77$.
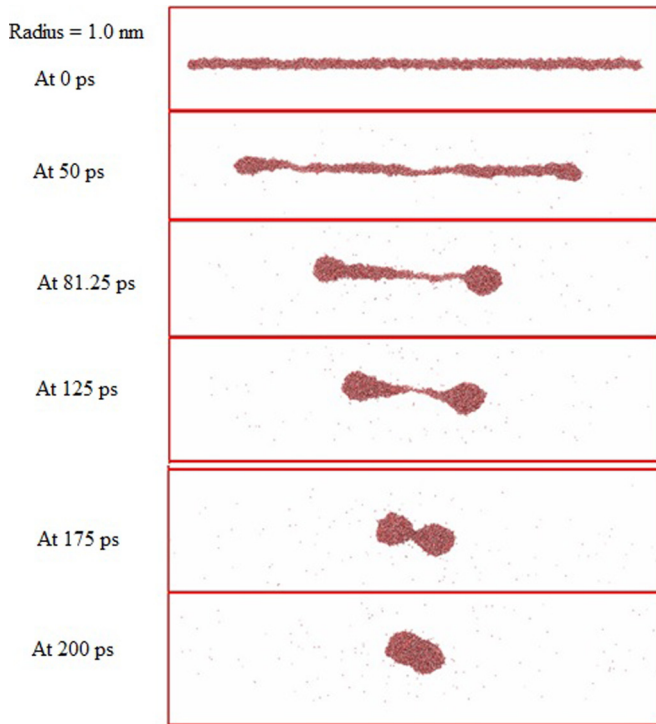
FIG. 11. The snapshots of MD trajectory from Case 10 (length is 90 nm and radius is 1 nm) with $E = 2900$ kV/cm at various time intervals.

2.35 D. A study by Jung *et al.* [36] have shown that, because of this permanent dipole moment, water molecules have extra energy while interacting with the external electric field $(\zeta \cdot E)$. To induce structural orderliness in liquid water, the energy due to the electric field $(\zeta \cdot E)$ has to be greater than the sum of the translational and rotational kinetic energy $(6k_B T/2)$ at 300 K. The minimum amount of electric-field strength required to induce the orderliness orientation is approximately 15 000 kV/cm.
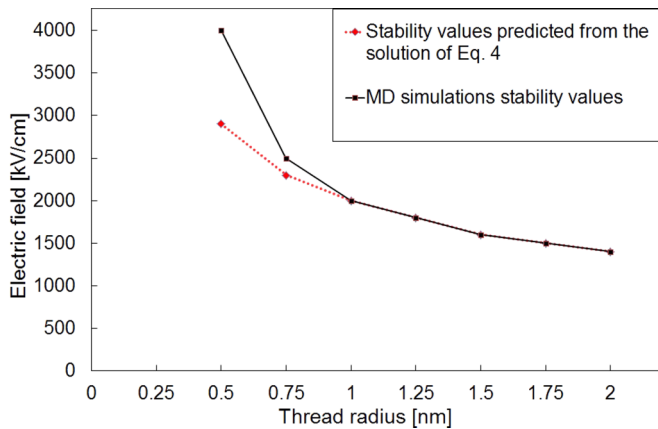
FIG. 12. Critical electric-field strength predicted from the solution of the dispersion relation and MD simulations for various thread radii.
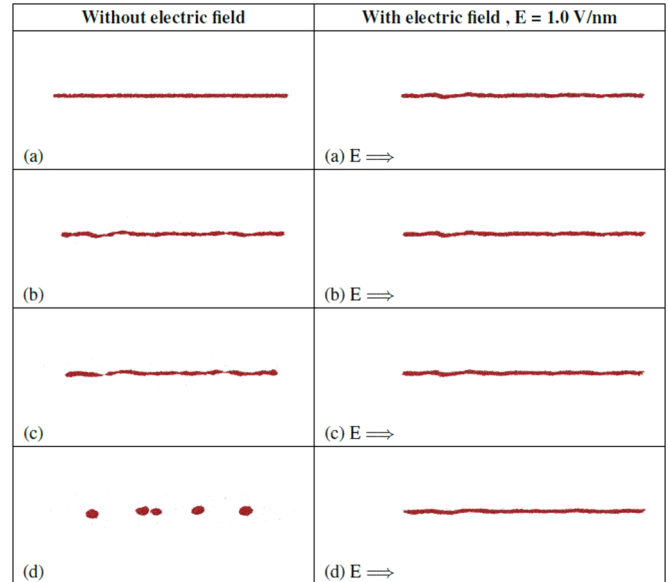

FIG. 13. The snapshots of MD trajectory for the liquid thread for the Case 10, at different time intervals. (a) 0 ps, (b) 15 ps, (c) 27.5 ps, and (d) 87.25 ps.

D. Effect of higher electric-field strength

The effect of higher electric-field strengths are studied by monitoring the local thread radius at various locations along its length. Figure 13 shows a typical case with an electric-field strength of 1 V/nm (for Case 10 given in Table III). The same without the electric field is also shown. The spatial variation of the thread radius along its axis for both cases (in the absence and presence of electric field) is shown in Figs. 14 and 15. It is seen that the thread radius diminishes to a minimum value near the pinch-off points (there are multiple pinch-off points at different time intervals) in the absence of an electric field but it fluctuates about its mean initial thread radius in the presence of an electric field. For both cases, the initial configurations are different in terms of local thread radius and this is attributed to the random velocity assigned during the equilibration phase.

At the nanoscale, the breakup is initiated due to the presence of thermal fluctuations which act as a perturbation imposed on the thread surface which can grow or decay
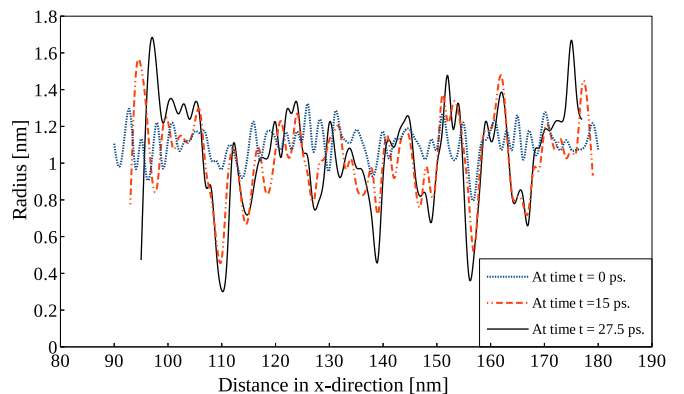

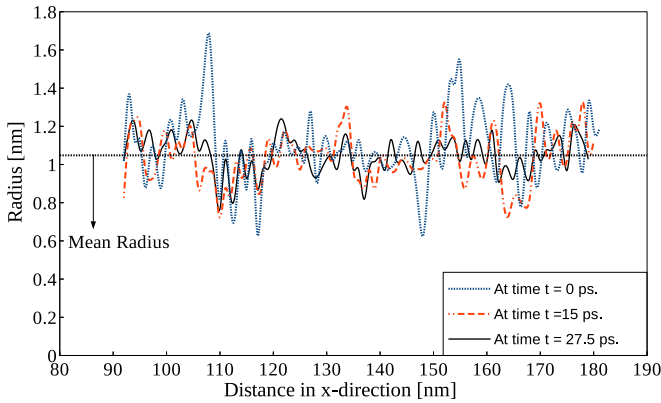FIG. 14. The spatiotemporal evolution of thread radius without electric field for Case 10.

FIG. 15. The spatiotemporal evolution of thread radius with electric field, $E = 10\,000$ kV/cm (1.0 V/nm) for Case 10.

in time. As seen from Figs. 13 and 15, it is clear that the axial electric field stabilizes the liquid nanothread. It can be said that the destabilizing effect caused by the presence of the thermal fluctuations are suppressed by the electric field and thus the stability of a liquid nanothread is enhanced. The theoretical hydrodynamic description of a nanoscale liquid jet or thread was first derived by Moseler and Landman [20]. They considered the effect of thermal fluctuations within the lubrication approximation applied to the Navier–Stokes equation for a macroscale jet or thread (resulting equation is known as the stochastic lubrication equations, SLEs) as

$$\rho(\dot{v}_0 + v_0 v_0') = -\gamma \kappa' + \frac{3\mu(h^2 v_0')'}{h^2} - \frac{(h\Upsilon)'}{h^2}\sqrt{\frac{6\mu k_B T}{\pi}}. \tag{7}$$

The above equation shows the effect of thermal fluctuations on the change in the local minimum radius (third term on the right-hand side of the SLEs). The temporal variation of the minimum radius is evaluated for an electric-field strength of 10 000 kV/cm (1.0 V/nm) at the same pinch-off location where the thread pinch-off took place for the first time without electric field for Case 10 (Fig. 6).

With the electric field acting, the radius of the thread is found fluctuating about the mean value of the initial radius
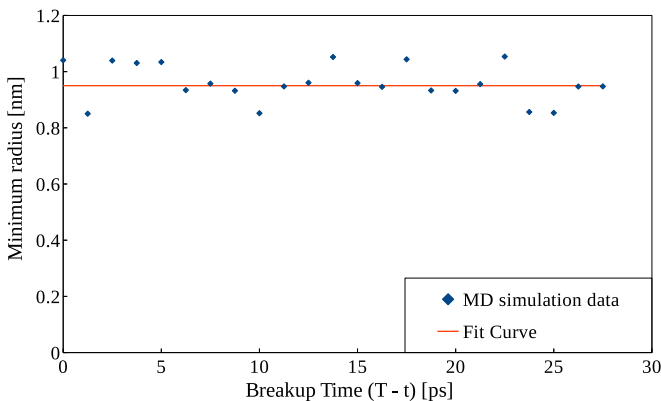

FIG. 16. Temporal variation of minimum radius for Case 10 ($L = 90$ nm and $r = 1$ nm at 300 K) with $E = 10\,000$ kV/cm.
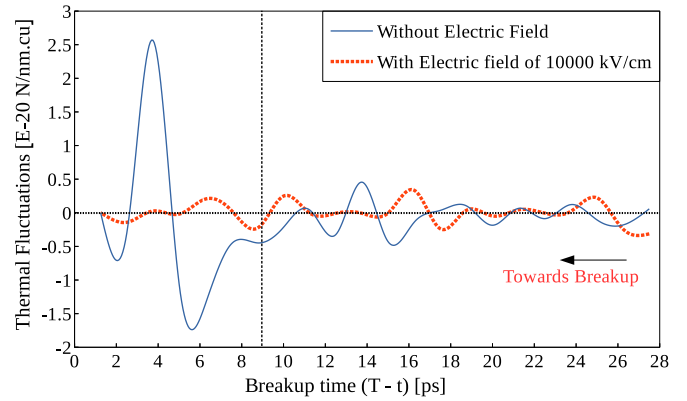

FIG. 17. Effect of electric field on thermal fluctuations.

(Figs. 15 and 16). At at a particular region, minimum radius is fluctuating about its initial radius at various time intervals (at the same pinch-off location and the time intervals considered for Case 10 without electric field). The variation of the thermal fluctuations calculated using Eq. (7) for both the cases (with and without electric field) is shown in Fig. 17. It can be seen that during the later stages of the breakup (9 ps before breakup) without electric field, the strength of thermal fluctuations increases, thereby increasing the rate of decrease of the minimum radius as shown in Fig. 6. But in the presence of the electric field, it is fluctuating about its mean value.

The surface tension is related to the Laplace pressure difference across the curved surface of a liquid thread or jet. This pressure difference causes the formation of the necking region in the thread or jet resulting in the breakup of a thread or jet. If we consider surface tension as a function of the applied electric field, the modified Laplace pressure difference without any free surface charge density can be written as

$$\Delta p = \gamma(E)\kappa - \frac{\varepsilon - \overline{\varepsilon}}{8\pi}E^2. \tag{8}$$

To understand the effect of electric field on surface tension and the resulting change in the thread dynamics, the pressure difference across the thread surface is calculated. Two cases are considered, i.e., a thread of 1 mm diameter and 2 nm diameter with electric field strength varying from 1 to
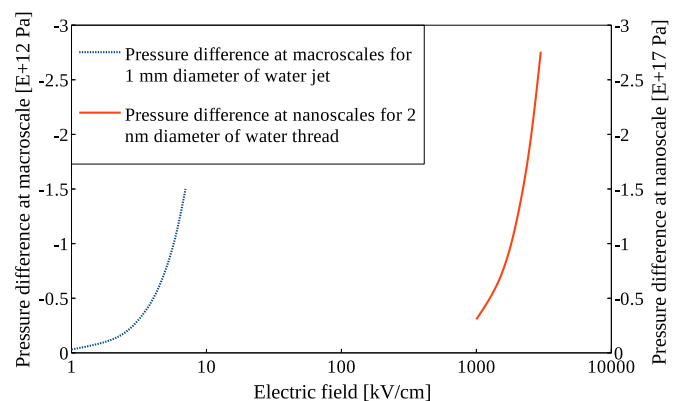

FIG. 18. Variation of Laplace pressure difference across the thread surface with surface tension as a function of E.
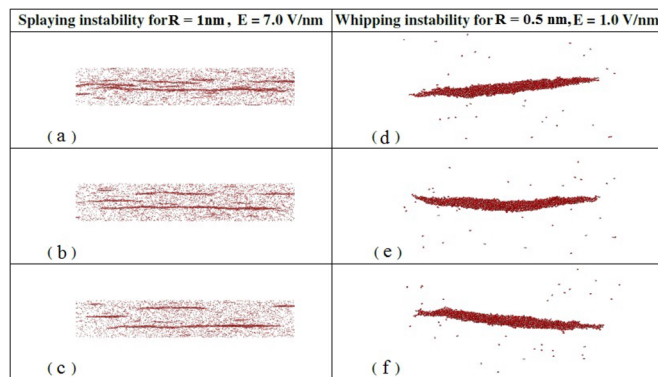
FIG. 19. Temporal evolution of a liquid thread for (left column) Case 10 and (right column) Case 8, at different time intervals with electric-field strength of 70 000 and 10 000 kV/cm. (a) 25 ps, (b) 50 ps, (c) 75 ps, (d) 77.5 ps, (e) 80 ps, and (f) 82.5 ps.

10 000 kV/cm (Fig. 18). Since the observed pressure difference is negative for both the cases, it may be concluded that the effect of electric field on surface tension does not play a significant role in liquid nanothread breakup.

For the molecular system under applied electric field, the total potential energy is the sum of the energies due to van der Waals interactions, Coulombic interactions, and dipole-moment interactions. Due to its inherent nature of the liquid water thread to remain at the minimum energy configuration, ratio of surface area to volume is reduced by these molecular forces leading to the breakup. But due to the polar nature of the liquid, the energy of the system can be minimized only if total Coulombic energy is also minimized. This can be achieved only by increasing surface area to the volume ratio. In the presence of electric field, the dipole moment interacts with the external electric field and increases the total energy of the system. Thus, the difference between these components of energy gives rise to the oscillatory motion about its longitudinal axis that is commonly known as the whipping instability [6]. For this study, the whipping instability is observed when the applied field strength is around 30 000 kV/cm. From the above viewpoint, it may be conceived that the whipping instability becomes significant when the ratio of surface area to volume is appreciable for a given liquid thread. The ratio of the surface molecules to the core molecules (SM/CM) at the end of the equilibration run for Cases 8 and 10 are 0.7029 and 0.2142, respectively. Thus whipping motion for the Case 8 is reported here for a field of 10 000 kV/cm in Figs. 19(d)–19(f).

As the electric-field strength is increased further, beyond the whipping-instability range, the length of the thread is found

to be reduced further. As a result of this, potential energy due to Coulombic interactions reaches a higher value. To be at the minimum energy state, the liquid thread disintegrates into thin ligaments instantaneously. This phenomenon occurs only when the applied electric field is strong enough to increase the total energy of the system. The observed phenomenon can be utilized for obtaining thin fibers with smaller dimensions (3 nm to 1 μm in diameter) and is commonly known as "splaying" [6]. For the present study, this occurs only for higher field strength in the range of 50 000 to 70 000 kV/cm. When the field strength is increased further, the liquid thread disintegrates and all the molecules move to the vapor phase. Figures 19(a)–19(c) show the effect of electric field on the splaying phenomena.

V. CONCLUSION

To study the effect of an axial electric field on the Rayleigh instability of a nanoscale liquid water thread, three-dimensional MD simulations are employed. The temperature of a liquid nanothread plays a significant role in determining the stability and the first breakup time of nanothreads. An increase in the temperature reduces the stability of a nanothread and thus the time taken for the first rupture decreases. The number of droplets formed increases with an increase in the temperature of the liquid. The solutions obtained from a dispersion relation developed by Hohman *et al.* [17] proves to be successful in predicting the dimensionless wave number, number of droplets, and critical electric-field strength for liquid nanothreads whose aspect ratio varies between 60 and 120. The results show that the axial electric field has a stabilizing effect by suppressing the Rayleigh instability even at the nanoscale. At a higher electric field, the cylindrical shape of the liquid nanothread is found to be retained and this stabilizing effect is due to the suppression of the thermal fluctuations. It is also observed that, when the electric-field strength is beyond the critical field strength, the phenomenon such as the whipping instability and the splaying instability are present. The present research could lead to the development of novel methods of controlling liquid nanostructures by using an electric field. This can be made useful in improving the processes like electrospinning.

[1] V. Menezes, S. Kumar, and K. Takayama, J. Appl. Phys. **106**, 086102 (2009).

[2] A. M. Kiper, Int. Commun. Heat Mass Transfer **11**, 517 (1984).

[3] H.-H. Lee, K.-S. Chou, and K.-C. Huang, Nanotechnol. **16**, 2436 (2005).

[4] D. J. Hayes, D. B. Wallace, and W. Cox, Proc. SPIE **3830**, 242 (1999).

[5] O. D. Sibailly, F. R. Wagner, L. Mayor, and B. Richerzhagen, Proc. SPIE **5063**, 501 (2003).

[6] D. Pisignano, *Polymer Nanofibers: Building Blocks for Nanotechnology* (The Royal Society of Chemistry, Cambridge, UK, 2013).

[7] F. Savart, Annal. Chim **53**, 337 (1833).

[8] L. Rayleigh, Proc. R. Soc. London **29**, 71 (1879).

[9] S. Tomotika, Proc. R. Soc. London, Ser. A **150**, 322 (1935).

[10] G. I. Taylor, Proc. R. Soc. London, Ser. A **146**, 501 (1934).

[11] J. Zeleny, Phys. Rev. **10**, 1 (1917).

[12] N. K. Nayyar and G. S. Murty, Proc. Phys. Soc., London **75**, 369 (1960).

[13] R. J. Raco, Science **160**, 311 (1968).

[14] G. Taylor, Proc. R. Soc. London, Ser. A **313**, 453 (1969).

[15] D. A. Saville, Phys. Fluids **13**, 2987 (1970).

[16] S. Sankaran and D. A. Saville, Phys. Fluids **5**, 1081 (1993).

[17] M. M. Hohman, M. Shin, G. Rutledge, and M. P. Brenner, Phys. Fluids **13**, 2201 (2001).

[18] J. Koplik and J. R. Banavar, Phys. Fluids **5**, 521 (1993).

[19] S. Kawano, Phys. Rev. E **58**, 4468 (1998).

[20] M. Moseler and U. Landman, Science **289**, 1165 (2000).

[21] J. Eggers, Phys. Rev. Lett. **89**, 084502 (2002).

[22] W. Kang and U. Landman, Phys. Rev. Lett. **98**, 064504 (2007).

[23] A. Tiwari, H. Reddy, S. Mukhopadhyay, and J. Abraham, Phys. Rev. E **78**, 016305 (2008).

[24] N. Gopan and S. P. Sathian, Phys. Rev. E **90**, 033001 (2014).

[25] S. Plimpton, J. Comput. Phys. **117**, 1 (1995).

[26] A. Stukowski, Modell. Simul. Mater. Sci. Eng. **18**, 015012 (2010).

[27] G. J. Guo and Y. G. Zhang, Mol. Phys. **99**, 283 (2001).

[28] G. J. Gloor, G. Jackson, F. J. Blas, and E. de Miguel, J. Chem. Phys. **123**, 134703 (2005).

[29] Y. Mao and Y. Zhang, Chem. Phys. Lett. **542**, 37 (2012).

[30] M. Orsi, Mol. Phys. **112**, 1566 (2014).

[31] F. H. Song, B. Q. Li, and C. Liu, Langmuir **29**, 4266 (2013).

[32] D. A. Saville, J. Fluid Mech. **48**, 815 (1971).

[33] Q. Jiang, Y. Chiew, and J. Valentine, Colloids Surf., A **83**, 161 (1994).

[34] A. Bateni, A. Amirfazli, and A. W. Neumann, Colloids Surf., A **289**, 25 (2006).

[35] J. Eggers and E. Villermaux, Rep. Prog. Phys. **71**, 036601 (2008).

[36] D. H. Jung, J. H. Yang, and M. S. Jhon, Chem. Phys. **244**, 331 (1999).